Iranian Journal of Materials Science and Engineering, Vol. 18, Number 2, June 2021
RESEARCH PAPER

Structural and Morphological Characterization of the Expanded Graphite Obtained by Ball Milling and HF Leaching

Saeid Karimi*, Akbar Heidarpour, Samad Ghasemi

* *s.karimi@hut.ac.ir*
* Department of Metallurgy and Materials Engineering, Hamedan University of Technology, Hamedan, Iran.

Received: January 2021 **Revised: March 2021** **Accepted: April 2021**
DOI: 10.22068/ijmse.2131

Abstract: *In this research, expanded graphite (EG) was successfully fabricated using a simple ball milling process followed by hydrofluoric (HF, 10 wt. %) leaching. The effect of ball milling time (0-15 h) and leaching time (1-24 h) on the exfoliation of graphite were examined by XRD and Raman spectroscopy. Furthermore, the morphological evaluation of the obtained expanded graphite samples was carried out by scanning electron microscopy (SEM). The XRD results of the ball-milled and HF treated samples showed a slight peak shift and broadening of (002) plane for expanded graphitein in comparison to the precursor and HF-treated samples. Moreover, the intensity of the (002) planes remarkably decreased by the ball milling process but remained constant after HF treatment. Raman spectra of the samples confirmed the ordering process only in HF-treated specimens. Moreover, the intensity ratio of $2D_1$ to $2D_2$ band gradually increased with enhancing the HF treatment time up to 5 hrs, indicating a decrement in the number of graphite layers by leaching in the HF solution*

Keywords: *Graphite, Ball milling, HF leaching, Expanded Graphite, Raman Spectroscopy.*

1. INTRODUCTION

Graphite is an inexpensive, environmentally friendly, and highly stable allotrope of carbon. It is a layered material consisting of covalently bonded carbon atoms in a hexagonal structure within the layer and a relatively weak force (e.g., van der Waals) exists between successive layers [1]. Until now, several methods have been introduced to synthesize expanded graphite. These methods are divided into two major groups, including top-down and bottom-up techniques. Chemical vapor deposition and expital growth belong bottom-up approaches, which can yield high-quality structures with a low density of defects [2, 3]. However, these techniques are expensive and can only be performed on a limited scale. Large-scale production with low cost can meet top-down methods, in which graphene is synthesized using graphite [4]. Comparing to conventional graphite, it is ideal for synthesizing graphene from expanded graphite due to the weak interaction between the graphite layer and more considerable interlayer distance [5]. In this process, graphene can be easily peeled by the exfoliation methods from expanded graphite layer by layer [6, 7]. It is worth mentioning that overcoming the van der Waals forces between graphene sheets has remained a challenge in the fabrication of graphene. In recent years, mechanical exfoliation [8], chemical exfoliation [9, 10], and electrochemical exfoliation [11, 12] methods have been developed to produce carbon-based material with a high specific area. Among the mentioned techniques, mechanical exfoliation has been extensively used to synthesize expanded graphite due to its accessibility and availability for large-scale production [13–15].

In general, there are two kinds of practical mechanical exfoliation routes to separate graphite layers, i.e., sonication assisted liquid phase [16] and ball milling [6]. However, sonication exfoliation can be easily performed on laboratory scale, and it has big challenging when establishing large-scale production. Furthermore, large-scale ultrasonic devices are generally expensive. In addition to the sonication-based exfoliation, dry and wet ball milling are the standard techniques that can be also used to expand the graphite layers by generating shear force. In wet ball milling, the sonication phenomenon can be occurred simultaneously with reducing the grain size. It has been reported that the milling of graphite an appropriate solvent by the planetary mill to separate the graphite layers. This process usually needs long-time milling and controlled milling speed to ensure predominant shear stress [4]. The significant challenge of milling exfoliation is the long-time processing and requirement of dispersion-assisted

[DOI: 10.22068/ijmse.2131]

solvents. The high-energy ball milling was used to reduce the size of graphite particles and induce mechanical energy of milling into elastic energy and defects in the powders. Therefore, the free Gibbs energy of nanocrystalline graphite will increase through the milling process. The storage energy of mechanically activated graphite resulted from the induced defects and structural disorder during the milling condition. Then, separating the graphite layers to obtain expanded graphite in HF solution can be easily achieved.

Several studies have been conducted in the field of co-ball milling graphite and solid polymers [17, 18]. Sun et al. [17] prepared expanded graphite by dry ball milling of graphite with cellulose. They have found that the dry ball milling graphite with cellulose can be a new method for the exfoliation of graphite in one step. A mass and straightforward production method for a few-layer graphite (graphene) is introduced by Leon et al. [18]. In this study, melamine (organic compound) is used as an additive in the milling process to produce large quantities and inexpensive graphene [18]. Another work in the field of mechanochemical treatment of graphite was introduced to exfoliate graphene. Different carbohydrates, including saccharose, fructose and, glucose, have been used for the successful exfoliation process during milling time [19]. It has been reported that expanded graphite is a noteworthy precursor for different applications such as synthesis graphene [20], graphene oxide [21], as well as a superior anode in Li-ions and Na-ions batteries [22, 23]. Therefore, fabrication of expanded graphite with specific features and on a large-scale can be desirable by simple methods like ball milling route.

Furthermore, structural and morphological features have been well characterized by different analyzing techniques [24, 25]. In addition to XRD analysis, Raman spectroscopy has been intensively employed to reveal detailed structural changes of carbon-based materials especially, their disordering and amorphization during the ball milling process [13, 14, 26, 27]. Raman spectroscopy is a non-destructive and high-resolution analysis for the characterization of the electronic, phononic, optical properties and the lattice structure of carbon-based materials [13]. Structural changes during ball milling and, HF treatment can also be confirmed by Raman spectroscopy. In addition to Raman characterization, this method has been extensively used to identify the impurities and defect density in the produced expanded graphite. As mentioned earlier, the defects and impurities have a significant role in the electronic structure of graphite, which undoubtedly changes the chemical, optical and, its related properties. This is why more important to carefully explore the structure variation by Raman spectroscopy.

The intensity ratio of D-band to G-band has been addressed as a phenomenological theory to calculate the concentrations of defects in the ball-milled graphite [28]. Additionally, the expanded graphite layers are interpreted in terms of I ($2D_1$)/ I ($2D_2$), derived from the Lorentzian curve fitting of the 2D-band of expanded graphite samples [29].

All of the studies as mentioned earlier addressed the synthesis of expanded graphite by the ball milling process. Moreover, wet exfoliation in the HF solution is a promising method to separate graphite sheets and generate expanded graphite [30, 31]. However, to the best of our knowledge, there have been no reports on the graphites characterization obtained by ball milling followed by HF treatment. In this study, expanded graphite (EG) was successfully fabricated using a simple ball milling process followed by immersion in 10 wt. % HF solution. In our method, the expanded graphite with high defect density and minimum impurities can be produced, in which the synthesis of expanded graphite can be easily scaled-up. The effects of milling time and leaching time on the crystal structure and Raman spectra were also examined.

2. EXPERIMENTAL PROCEDURE

The analytical grade graphite (99.7% <200 μm) was used as starting material after being dried in air at 95 °C for 12h. 2 g of graphite was ball milled with stainless steel container Retch PM100 planetary ball mill. The ball to powder weight ratio was set at 20:1 and, the rotation speed was 400 r/min. The milling time was ranged from 5 to 15h. Then, 0.5 g of the ball-milled powders were leached in 50 mL of HF solution (10 wt. %) and stirred for 10 min. Afterward, the pulp was kept at various time intervals (1, 5, 24 h). The samples were then washed several times with distilled water. The samples' codes are listed in Table 1.

The phase of the samples was analyzed by X-ray

[DOI: 10.22068/ijmse.2131]

diffraction (XRD) using an Asenware AW-DX300 diffractometer equipped with a Cu (K_α) radiation source (λ=0.154056 nm). The data obtained from this analysis were evaluated by X'pert HighScore Plus software. The morphology of the ball-milled and HF-treated powders was assessed by scanning electron microscopy (SEM, Quanta200, FEI). Raman spectroscopy was also performed at room temperature using a LabRam microsetup system in backscattering geometry.

Table 1. The code of samples

Time of HF leaching (h)	Time of ball milling (hours)			
	0	5	10	15
0	G	B5	B10	B10
1	H1	B5H1	B10H1	B15H1
5	H5	B5H5	B10H5	B15H5
24	H24	B5H24	B10H24	B15H24

3. RESULTS AND DISCUSSION

The XRD pattern of the precursor (G) and the samples leached in HF for 1h (H1) and 24h (H24) without milling are presented in Fig. 1. All diffraction peaks in the XRD patterns can be indexed to the pure hexagonal phase of the graphite structure (JCPDS No. 00-025-0284). The patterns show two dominant characteristic peaks of the graphite (around 2θ=26.6° and 54.8°), which can be assigned to (002) and (004) planes, respectively [32]. As can be seen in Fig. 1, the HF leaching of graphite did not make a significant difference in diffraction peaks of H1 and H24 patterns.

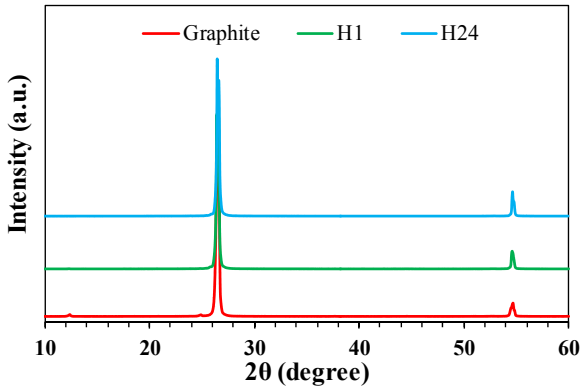

Fig. 1. XRD patterns of graphite precursor samples obtained after 1 and 24h HF leaching for 1h.

In this study, graphite powders were ball milled for 5 to 15h and subsequently leached in HF solution to determine the effect of such treatments on the structure and formation of expanded graphite. Fig. 2 shows the XRD patterns of the sample ball milled for 15h and after leaching in HF solution (B15H1 and B15H24); the XRD patterns of graphite are also presented in this figure. Additionally, the magnified XRD patterns of B15H1 and B15H24 samples are also depicted in Fig. 2. As can be seen, the ball milling process resulted in a slight peak shift, broadening, decreasing intensity of the (002) plane. The expanded graphite powders exhibited almost the same diffraction peaks position at ca. 26.5° as those of graphite, suggesting that the expanded graphite still retained the structure of the carbon atoms. The characteristic (002) peak of the pristine graphite at 26.6° has an interplanar distance, d_{200}, of 0.335 nm, implying that the graphite is a highly orientated carbon material [33]. After ball milling and HF treatment, the d-spacing of B15H1 and B15H24 remained almost unchanged (0.336 nm).

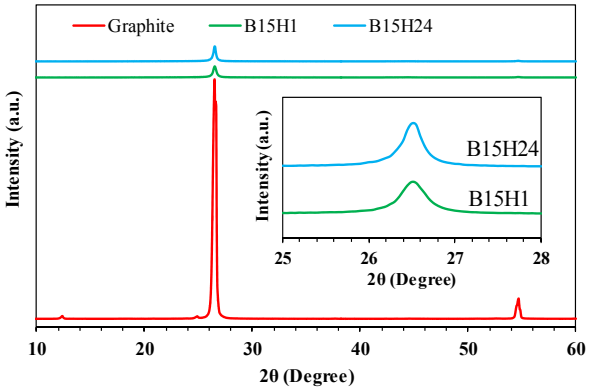

Fig. 2. XRD patterns of graphite precursor, B15H1 and B15H24 samples.

Furthermore, the sharp peak in the XRD pattern of B15H1 and B15H24 shows that it comprises a large number of layers [34]. In addition to the minor shift of the (002) peak from 26.6° to 26.5°, its intensity also declined and started significant broadening. It should be mentioned that an aggressive HF leaching step removed all impurities such as iron and iron oxides phases that might enter during the ball milling process. Besides, the reduction in grain size through the ball milling process can be the main reason for a decrement of peak intensities [17].

Furthermore, the intensity ratio of the (002) to (004) diffraction plane ($I_{(002)}/I_{(004)}$) was measured

[DOI: 10.22068/ijmse.2131]

for G, H1, H24, B15H1, and B15H24 samples and plotted in Fig. 3(a). For precursor graphite, the ratio was equal to c.a. 11.02. In HF treatment, this value was decreased to 8.53 and 4.5 for H1 and H24, respectively. This shows that an increment in HF treatment time up to 24h will result in a gradual in the intensity of the (002) planes. However, the intensity ratio is extremely revered by ball milling before the HF treatment. It should be noted that the value of intensity ratio is found to have a relatively large error of c.a. ±3%, which can be assigned to the uncertainty of the background measurement of the diffraction profile. Nevertheless, the variation in intensity ratio ($I_{(002)}/I_{(004)}$) of samples was much more than ±3% error [35]. The calculated intensity ratio can be used to derive valuable information about interlayer displacement. In other words, the higher ratio of $I_{(002)}/I_{(004)}$, the more crystallinity of the carbon samples [35]. At the constant value of d-spacing (3.35 Å), $I_{(200)}/I_{(004)}$ of G was about 11.02, which declined to 8.53 for H1, implying that precursor graphite (G) has a much larger average atomic displacement than H1. As a result, HF treatment caused a long-range order of carbon samples. In return, ball milling and HF treatment of the samples may lead to the decrement of the crystallinity degree and hence the accumulation of structure defects [36]. It has been reported that defect density increases by milling in ball-milled graphite lattice, increasing the oxygen content as the defect sites. This phenomenon would be favored sites for the synthesis of high oxygen density in graphene oxide [37]. Thus, our method can be a right candidate for the fabrication of a large-scale graphite with high defect density.

The intense and sharp diffraction peaks in the XRD pattern confirmed the high crystallinity of graphite. For further understanding, the intensity to FWHM ratio of the (002) plane at 26.5° for G, H1, H24, B15H1, and B15H24 samples was calculated and depicted Fig. 3(b).

As shown in Fig. 3(c), the crystallinity of G, H1, H24, B15H1, and, B15H24 samples were 89.2%, 88.1%, 86.8%, 58.5% and 55.6%, respectively. The crystallinity of the HF-treated samples (H1 and H24) was slightly decreased by enhancing the HF leaching time. On the contrary, the degree of crystallinity of the ball-milled and HF-leached samples (B15H1 and B15H24) was drastically dropped, suggesting a reversion to a more short-range ordered state away from the equilibrium state [38]. In comparison, more prolonged milling from 1 to 24 hours, the crystallinity of expanded graphite does not show a significant decrease. These results seem to contradict the finding of Zhang et al. [38], who expressed that the ball milling process increased the crystallinity degree of graphitized carbon black (GCB).

Based on our results, the peak intensity of carbon

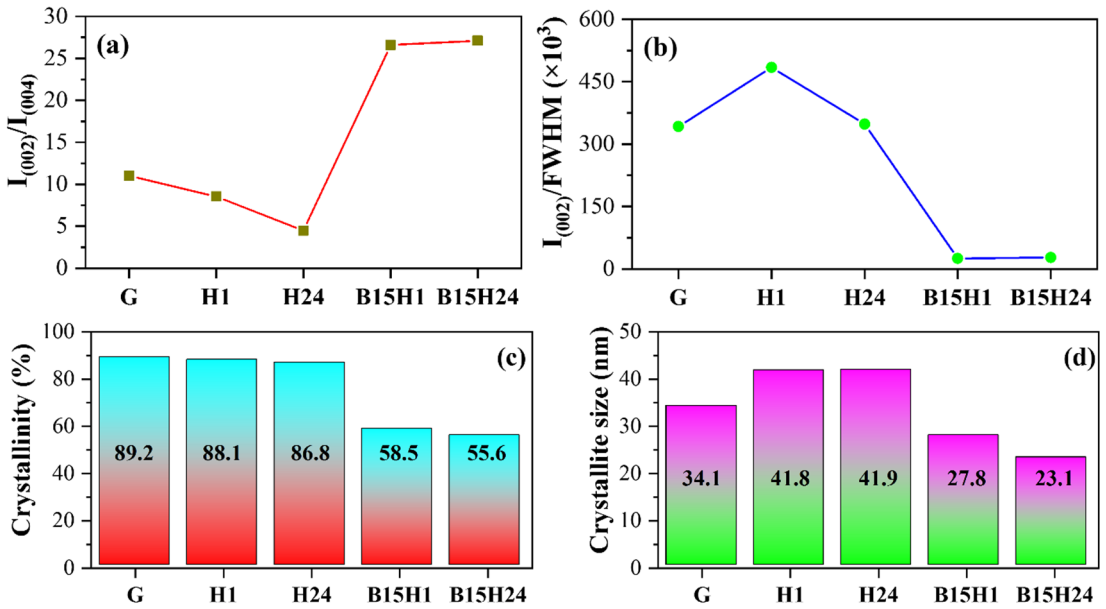

Fig. 3. (a) Changes of intensity ratio $I_{(002)}/I_{(004)}$, (b) the ratio intensity to FWHM of the (002) plane's peak at 26.6°, (c) crystallinity and (d) crystallite size of different samples.

[DOI: 10.22068/ijmse.2131]

materials was significantly reduced upon ball milling treatment [39–42].

Fig. 3(d) depicts the crystallite size of G, H1, H24, B15H1, and B15H24 samples. Overall, the leaching process in HF acid solution results in the growth of crystallite size (i.e., H1 and H24 samples). While milling the graphite before HF-treatment seems to be very effective in reducing the size of crystals. A minor decrement of crystallite size by rising HF leaching time (i.e., 27.8 nm for B15H1 to 23.1 nm for B15H24) can be seen, suggesting that longer HF treatment causes to growth of new crystals from high defect zone. According to Sun et al. [17] results, milled graphite showed a reduction in crystallinity and crystal size. The crystallite size of graphite decrease from 100 µm to 12 µm and, a 20% reduction in the crystallinity of milled graphite is obtained after 24 hours milling process. These findings are in close agreement with the results of our study.

Fig. 4 shows the Raman spectra of precursor (graphite) and samples leached in HF for 1, 5, and 24h (H1, H5, and H24). The graphite Raman spectrum showed general features in the range of 1000-3000 cm^{-1} as D, G, and, 2D peaks emerged at 1348.8, 1584.6, and 2736 cm^{-1}, respectively.

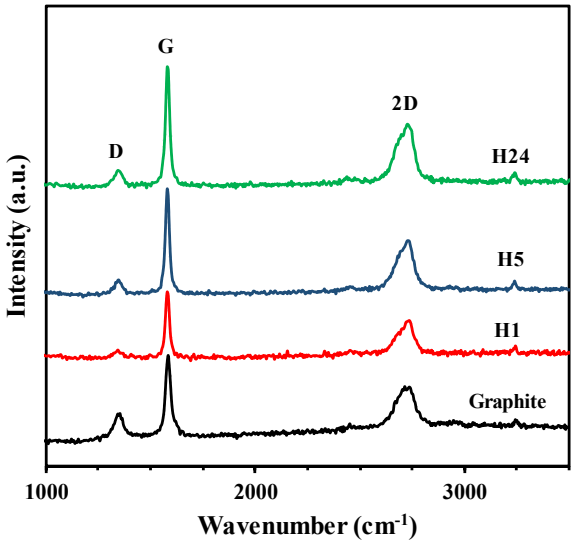

Fig. 4. Raman spectra for precursor (graphite) and leached samples in HF for 1, 5 and 24h (H1, H5 and H24).

The D peak is due to the breathing modes of sp^2 atoms, and it requires a defect for its activation. The D band comes from A_{1g} ring breathing mode and importantly, this mode is symmetrically forbidden in perfect graphite [14, 43]. Therefore, the intensity of the D peak in the Raman spectrum of the sample is attributed to the extent of disorder and defects [44]. The second order of zone boundary phonons gives rise to the 2D peak and, it has been attributed to the first overtone of the D peak. Note that even if the D peak is absent, the 2D mode is always present as defects are not necessary to activate two phonons.

On the other hand, the D peak requires defects for activation, while the overtone originates from a process in which the momentum can be always conserved by two phonons with opposite wave vectors [45]. Furthermore, defects induce a significant increase in the intensity of the D band while decreasing the 2D peak height intensity with line broadening. The strong G peak is attributed to the doubly degenerate one center E_{2g} mode. It is due to sp^2 bonded carbon from the carbon-carbon double generates stretching modes in the hexagonal layers.

Important information on the electronic structure of graphite and leached samples can also be derived from the Raman peak position [46]. In HF-treated samples (H1, H5, and H24) exhibited a redshift by 5 cm^{-1} from 1584.6 cm^{-1} for the precursor to 1579.5 cm^{-1}. This redshift can be due to the interaction of the HF solution with graphite, which is necessary for charge transfer during the leaching process.

Additional information about the carbon materials can be obtained by analyzing the ratio of the intensities of the individual peaks. As an example, the defect density of the graphite and HF-treatment samples can be deduced from the I_D/I_G ratio. According to Table 2, D to G peak (I_D/I_G) exhibited a two-fold drop upon HF treatment from 0.469 in the precursor to 0.207 in H1, implying an ordering process.

Table 2. The intensity of D to G peak (I_D/I_G) of precursor and H1, H5 and H24 samples.

samples	Precursor	H1	H5	H24
I_D/I_G	0.469	0.256	0.212	0.207

The value of I_D/I_G decreased with prolonged HF leaching by 16% before reaching almost constant conditions during extended HF leaching up to 24h. This means that the ordering process stops by increasing the HF leaching time from 5 to 24 h. These results are in formal agreement with Bokobza et al. [47], who reported two prominent bands at 1581 (G) and 2678 cm^{-1} (2D) for highly-oriented pyrolytic graphite.

[DOI: 10.22068/ijmse.2131]

The curve fitting of the 2D peak of samples was done using the Lorentzian distribution. The 2D band was decomposed into two peaks of $2D_1$ and $2D_2$ at around 2660 cm^{-1} and 2720 cm^{-1}, respectively. While the 2D Raman band in single-layer graphite can be fitted with a single component, graphites with more than one layer can be best fitted to two components ($2D_1$ and $2D_2$). The results can be explained in terms of double resonance Raman scattering [29], which indicates the electronic structure of graphite is captured in its 2D Raman spectra. Furthermore, the intensity of the $2D_1$ band is usually less than the $2D_2$ band, whereas, for the bilayer, the two peaks have almost the same intensity. An increase in the number of graphite layers leads to a growth in the intensity of the $2D_2$ band (high-frequency component) compared to the $2D_1$ band [29]. Fig. 5 shows the raw data and Lorentzian-fitted results of the 2D band for precursor (G) and HF-leached samples (H1, H5, and H24). $2D_1/2D_2$ ratio gradually increased by enhancing the HF treatment duration up to 5 hours, indicating a decrement in the graphite layers upon leaching in HF. The $2D_1/2D_2$ ratio of H24 again decreased probably due to the dissolution of graphite layers upon long-term HF treatment.

As shown in Fig. 6, Raman spectra of graphite which were ball milled and then leached in HF, revealed three fundamental bands, D-band (1348.8 cm^{-1}), G-band (1579.5 cm^{-1}), and 2D-band (2714 cm^{-1}). Apart from these prominent peaks, another peak, D', emerged at around 1630 cm^{-1} reflecting the presence of defects. This band rose together with the G band and can be considered as the shoulder peak for the G band [48]. It appears only in cases with a high density of defects [26, 49]. It can be concluded that the difficult ball milling process led to the formation of the high-density defects in the graphite crystals. It has been known that material with a high specific area, i.e., expanded graphite and graphene, could be used in different applications such as gas sensors, batteries for energy storage, optoelectronic and electronic devices. Nevertheless, it is worthwhile to mention that presence of defects in the structure is almost mandatory for having better and more performance [50].

Fig. 7 depicts the plot of D/G vs. the ball milling time for samples experiencing HF treatment for 1h, 5h, and 24h.

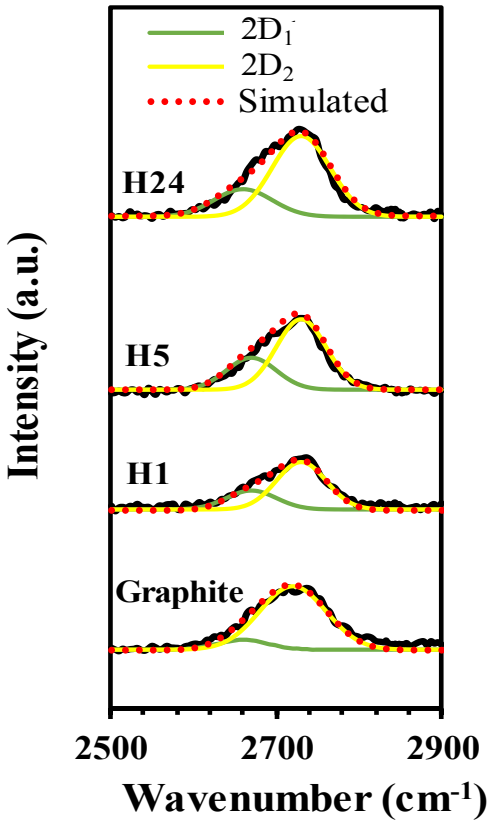

Fig. 5. The fitting results of 2D band of Raman spectra of precursor (graphite) and leached samples in HF for 1, 5 and 24h (H1, H5 and H24).

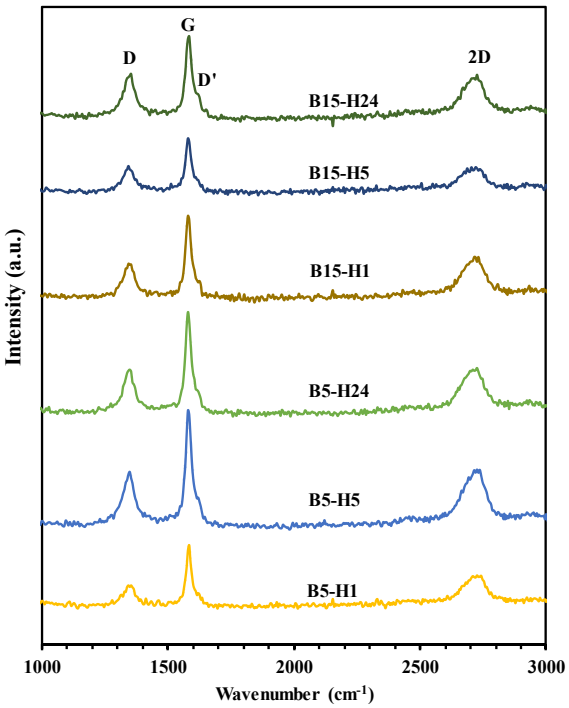

Fig. 6. Raman spectra of ball milled graphite and subsequently leached in HF solution.

[DOI: 10.22068/ijmse.2131]

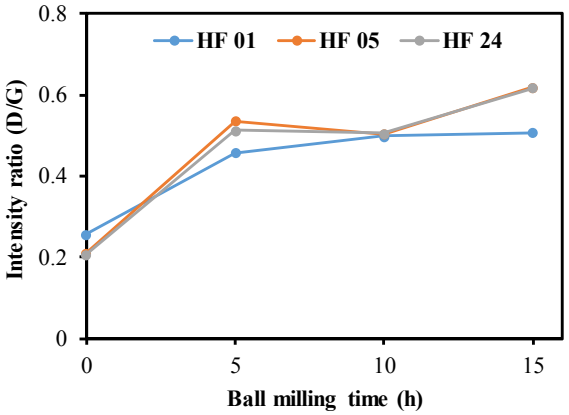

Fig. 7. Intensity ratio of D-band to G-band of the graphite samples ball-milled and HF treated for various times.

For the samples leached for an hour (HF 01) after 0, 5, 10, and 15 hours of ball-milling, the D/G ratio increased from 0.25 for H1 to 0.46 for B5H1. Followed by a 0.04 increment in B10H1 compared with B5H1, it finally reached stable conditions during extended HF leaching to 24h (B15H1). For the samples which were leached for 5 hours (HF 05), the plot showed a severe increase from 0.21 for the H5 sample to 0.53 for the B10H5. Then, it remained almost constant at 0.20 upon prolonged milling times up to 10 h; then, it started to increase again for milling times of 15 h (B15H5). The same trend can be found for samples that were HF-treated for 24 h. As mentioned above, the I_D/I_G ratio can describe the extent of defects, and crystallinity of the expanded graphite before and after ball milling followed by HF treatment. The I_D/I_G ratios of the B15H5 and B15H24 were significantly higher than those of the other samples reflecting a relatively higher density of defects and lower crystallinity in comparison with the highly-oriented structure [49].

In conventional wet milling, impurities such as iron, iron oxide and even zirconium oxide particles can enter final carbon-based products [51]. Based on the investigation of González et al. [19], if there are two distinct processes, i.e., ball milling and HF treatment through the expanded graphite synthesis, most soluble impurities can dissolve in the solution. Therefore, the expanded graphite with high defect density can be easily prepared by a simple method.

Table 3 illustrates the intensity ratio of $2D_1$ band to $2D_2$ band for ball-milled graphite, which was then HF-leached. These values were obtained by fitting Lorentzian data to the 2D band. Generally, this ratio exhibited a gradual enhancement with increasing the HF-treatment time at constant ball milling time. For instance, the intensity of $2D_1$ to $2D_2$ increased from 0.197 for B5H1 to 0.307 for B5H24. On the other hand, the prolonged leaching time resulted in fewer layers of expanded graphite. Therefore, the B5H1 sample possessed more layers compared to B5H24. The same trend was observed in this study in the case of the ball-milled graphite (for 10 and 15 h).

The morphology of precursor graphite is demonstrated in Fig. 8(a) and (b). As shown in Fig 8(a), precursor graphite contained many thin flakes whose thickness was mostly below 2 µm. The graphite particles before milling and leaching in HF solution illustrate a smooth surface with flake morphology. Furthermore, the SEM micrograph shows the actual particle size range of 2.3-13.1 µm. Besides, the SEM micrograph at higher magnification demonstrates the compact structure of the starting graphite packing with minor porosity. Besides, Fig. 8 illustrates the SEM micrograph of the expanded graphite samples including, B15H1 (c), B15H5 (d), and B15H24 (e).

It is observed that after applying the milling and HF treatment processes into the graphite powders, graphite interlayers gradually expanded upon prolonged HF treatment. The high magnification of the FESEM micrograph demonstrated an increment in the graphite flakes interlayer spacing due to the separation of layers leading to the porous structure. A decrease in the intensity of the (004) plane and crystallinity legally confirmed the destruction of the graphite crystal structure through the ball milling process followed by HF leaching (see Fig. 3(a) and (c)).

Table 3. The intensity ratio of $2D_1$ band to $2D_2$ band of ball-milled and subsequently leached graphite

Samples	B5H1	B5H5	B5H24	B10H1	B10H5	B10H24	B5H1	B15H5	B15H24
$I(2D_1)/I(2D_2)$	0.197	0.186	0.307	0.275	0.286	0.340	0.238	0.270	0.373

[DOI: 10.22068/ijmse.2131]

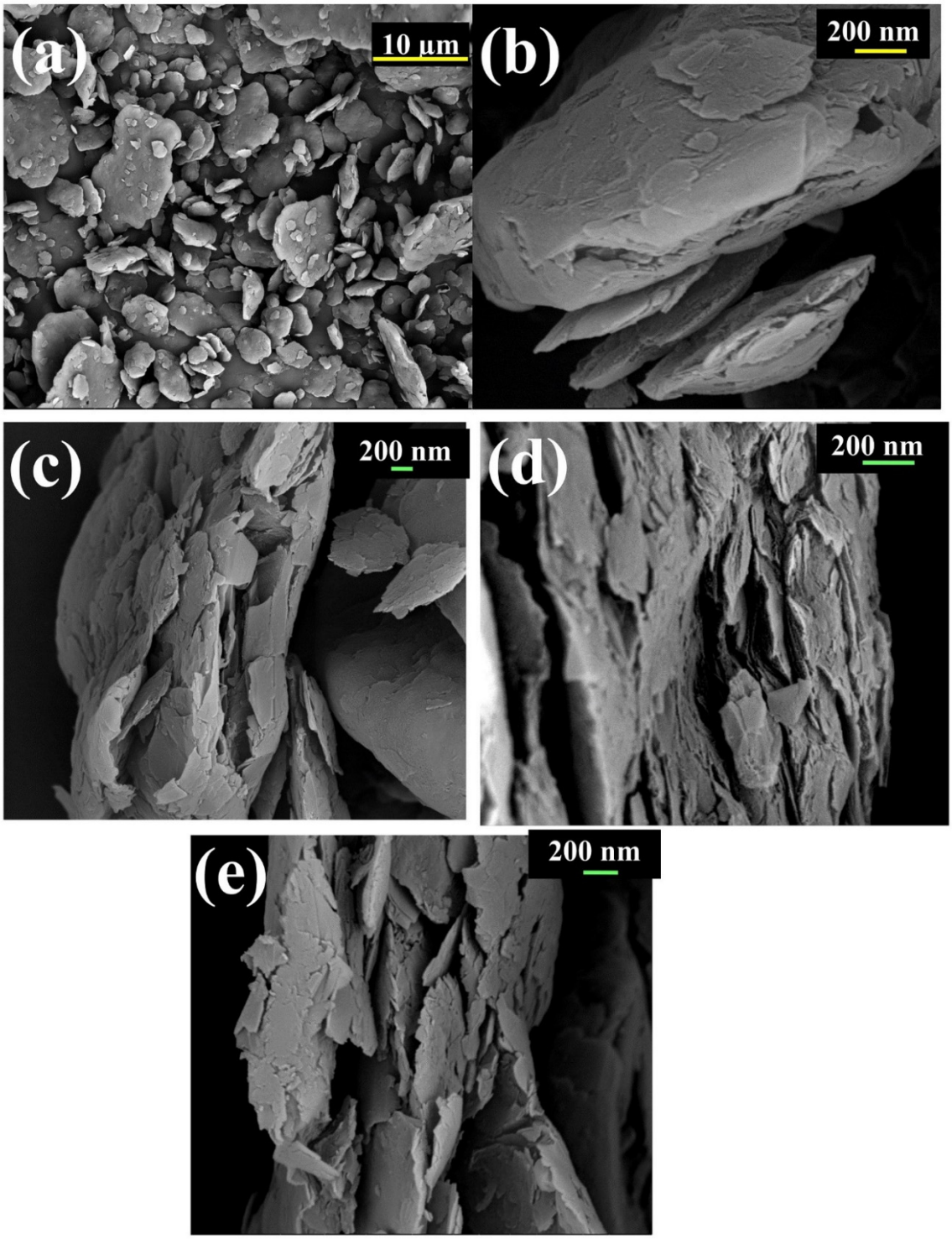

Fig. 8. (a) SEM micrographs and (b) high-magnification of as-received graphite and FESEM images of expanded graphite (c) B15H1, (d) B15H5, and (e) B15H24.

As shown in SEM images, the expanded graphite (B15H1, B15H5, and B15H24) possessed a loose and porous structure consisting of many graphite layers of a few nanometers thickness.

Moreover, these findings confirm the Raman results in which prolonged more ball milling and HF treatment resulted in the higher intensity ratio of $2D_1$ to $2D_2$. As seen in Fig. 8(c)-(e), the

[DOI: 10.22068/ijmse.2131]

thickness of expanded graphite particles was lower than 10 nm. Furthermore, Antisari et al. [52] have been reported that ball milling of graphite can yield nano-sheets with a thickness of lower than 10 nm. Moreover, it is well established that expanded graphite can be well exfoliated in the direction of the c-axis [53], which is fairly in agreement with obtained results in this study.

Fig. 9 demonstrates the FESEM image of the expanded graphite samples, which are obtained after 5 and 15 hours of milling and subsequently HF leaching for 24 hours. The images of both samples (i.e., B5H24 and B14H24) illustrate irregular shapes with rough surfaces. According to the FESEM image in Fig. 9, an increment in the milling time increases in interlayer spacing of expanded graphite. The most important reason are induced surface defects and residual stress during milling process, which will increase by elongated milling. In addition, the Fe atom can be introduced into the graphite structure during the milling process. As milling is increased, the higher concentration of Fe can inter the structure. In the HF leaching stage, iron atoms can exit from the graphite structure and cause an increase in interlayer spacing of expanded graphite. Therefore, a longer milling time will be a very effective way in obtaining an expanded and porous structure.

4. CONCLUSIONS

In this study, expanded graphite (EG) was successfully fabricated using a simple ball milling process followed by leaching in a 10 wt. % hydrofluoric (HF) solution.

The effect of two parameters, including ball milling time and HF-leaching time on the crystal structure, morphology, and Raman spectra of the samples, was examined. The milling time was varied in the range of 0 to 15 h, while the leaching time was changed in the range of 1-24 h. The results showed that only HF leaching was in favor of the structural ordering of graphite and minimizing the density of defects. On the contrary, the ball-milled powders showed more disorder, in agreement with the considerable amount of defects in the expanded graphite structure.

The evaluation of the I ($2D_1$)/I ($2D_2$) ratio revealed that the more leaching time would result in fewer layers of graphite in the ball-milled samples. SEM images showed an increase in the graphite flakes interlayer spacing due to an increment in the distance which led to porous structure. Also, it is fair to mention that the proposed method can be a superior candidate for the synthesis expanded graphite on a large-scale.

5. REFERENCES

[1] Yoshimoto, S., Amano, J., Miura K., "Synthesis of a fullerene/expanded graphite composite and its lubricating properties." J. Mater. Sci., 2010, 45, 1955–1962.

[2] Strupinski, W., Grodecki K., Wysmolek A., Stepniewski, R., Szkopek, T., Gaskell, P. E. "Graphene epitaxy by chemical vapor deposition on SiC." Nano Lett., 2011, 11, 1786–1791.

[3] Zhang, Y., Zhang, L., Zhou, C., "Review of chemical vapor deposition of graphene

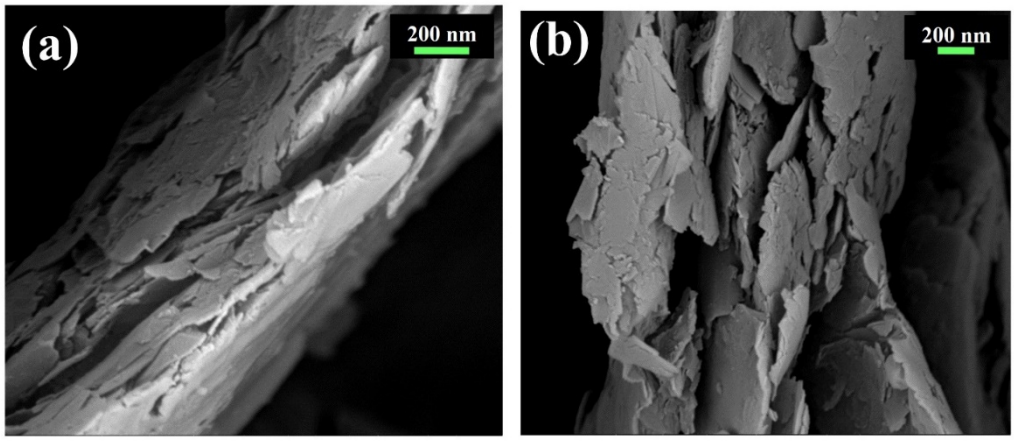

Fig. 9. FESEM images of expanded graphite (a) B5H24 and (b) B15H24.

[DOI: 10.22068/ijmse.2131]

and related applications." Acc. Chem. Res., 2013, 46, 2329–2339.
[4] Yi, M., Shen, Z., "A review on mechanical exfoliation for the scalable production of graphene." J Mater. Chem. A., 2015, 3, 11700–11715.
[5] Zhu, L., Zhao, X., Li, Y., Yu, X., Li, C., Zhang, Q., "High-quality production of graphene by liquid-phase exfoliation of expanded graphite." Mater. Chem. Phys., 2013, 137, 984–990.
[6] Posudievsky, O. Y., Khazieieva, O. A., Koshechko V. G., Pokhodenko, V. D., "Mechanochemical Delamination of Graphite in the Presence of Various Inorganic Salts and Formation of Graphene by Its Subsequent Liquid Exfoliation." Theor. Exp. Chem., 2014, 50, 103–109.
[7] Kumar, R., Bhargava, P. "In situ-growth of silica nanowires in ceramic carbon composites." J Asian Ceram. Soc., 2017, 5, 304–312.
[8] Cai, M., Thorpe, D., Adamson, D. H., Schniepp, H. C., "Methods of graphite exfoliation." J. Mater. Chem., 2012, 22, 24992–25002.
[9] Adelkhani, H., Didehban, K., Dehghan, R., "Fabrication and characterization of polyaniline-graphene composite as electrode in electrochemical capacitor." Iran J. Mater. Sci. Eng., 2016, 13, 29–34.
[10] Foroutan, S., Hashemian, M., Khandan, A., "A novel porous graphene scaffold prepared using Freeze-drying technique for orthopedic approaches, abrication and buckling simulation using GDQ method." Iran J. Mater. Sci. Eng., 2020, 17, 62–76.
[11] Coroş, M., Pogəcean, F., Roşu, M., C., Socaci, C., Borodi, G., Mageruşan, L., Biriş, A. R., Pruneanu, S., "Simple and cost-effective synthesis of graphene by electrochemical exfoliation of graphite rods." RSC Adv., 2016, 6, 2651–2661.
[12] Lim S., Han J., H., Kang H., W., Lee, J. U., Lee, W., "Preparation of electrochemically exfoliated graphene sheets using DC switching voltages." Carbon Lett., 2020, 30, 409–416.
[13] Wu, J. B., Lin, M. L., Cong, X., Liu, H. N., Tan, P. H., "Raman spectroscopy of graphene-based materials and its applications in related devices." Chem. Soc. Rev., 2018, 47, 1822–1873.
[14] Xing, T., Li, L. H., Hou, L., Hu, X., Zhou, Sh., Peter, R., Petravic, M., Chen, Y., "Disorder in ball-milled graphite revealed by Raman spectroscopy." Carbon, 2013, 57, 515–519.
[15] Hasani, A., Do, H. H., Tekalgne, M., Hong, S. H., Jang, H. W., Kim, S. Y., "Recent progress of two-dimensional materials and metal–organic framework-based taste sensors." J. Korean Ceram. Soc., 2020, 57, 353–367.
[16] Yi, M., Shen, Z., Ma, S., Zhang, X., "A mixed-solvent strategy for facile and green preparation of graphene by liquid-phase exfoliation of graphite." J. Nanoparticle Res., 2012, 14, 1003.
[17] Sun, P., Kuga, S., Wu, M., Huang, Y., "Exfoliation of graphite by dry ball milling with cellulose." Cellulose, 2014, 21, 2469–2478.
[18] León, V., Quintana, M., Herrero, MA., Fierro, J. L. G., Hoz, A. D. L., Prato, M., Vázquez, E., "Few-layer graphenes from ball-milling of graphite with melamine." Chem. Commun., 2011, 47, 10936–10938.
[19] González, VJ., Rodríguez, AM., León, V., Frontiñán-Rubio, J., Fierro, J. L. G., Durán-Prado, M., Muñoz-García, A. B., Pavone, M., Vázquez, E., "Sweet graphene, Exfoliation of graphite and preparation of glucose-graphene cocrystals through mechanochemical treatments." Green Chem., 2018, 20, 3581–3592.
[20] Liao, K., Ding W., Zhao, B., Li, Z., Song, F., Qin, Y., Chen, T., Wan, J., Han, M., Wang, G., Zhou, J., "High-power splitting of expanded graphite to produce few-layer graphene sheets." Carbon, 2011, 49, 2862–2868.
[21] Yang, H., Li, H., Zhai, J., Sun, L., Yu, H., "Simple synthesis of graphene oxide using ultrasonic cleaner from expanded graphite." Ind. Eng. Chem. Res., 2014, 53, 17878–17883.
[22] Wen, Y., He, K., Zhu, Y., Han, F., Xu, Y., Matsuda, I., Ishii, Y., Cumings, J., Wang, C., "Expanded graphite as superior anode for sodium-ion batteries." Nat. Commun., 2014, 5, 4033.
[23] Lin, Y., Huang, ZH., Yu, X., Shen, W., Zheng, Y., Kang, F., "Mildly expanded

[DOI: 10.22068/ijmse.2131]

graphite for anode materials of lithium ion battery synthesized with perchloric acid." Electrochim. Acta. 2014, 116, 170–174.

[24] Geim, AK., MacDonald, A. H. "Graphene: Exploring carbon flatland." Phys Today., 2007, 60, 35–41.

[25] Borah, M., Dahiya, M., Sharma, S., Mathur, R. B., Dhakate, S. R., "Few Layer Graphene Derived from Wet Ball Milling of Expanded Graphite and Few Layer Graphene Based Polymer Composite." Mater. Focus, 2014, 3, 300–309.

[26] Ferrari, A. C. "Raman spectroscopy of graphene and graphite: Disorder, electron-phonon coupling, doping and nonadiabatic effects." Solid State Commun, 2007, 143, 47–57.

[27] Pimenta, M. A., Dresselhaus, G., Dresselhaus, MS., Cançado, L. G., Jorio, A., Saito, R., "Studying disorder in graphite-based systems by Raman spectroscopy." Phys. Chem. Chem. Phys., 2007, 9, 1276–1291.

[28] Ferrari, A., Robertson J. "Interpretation of Raman spectra of disordered and amorphous carbon." Phys Rev B - Condens. Matter. Mater. Phys., 2000, 61, 14095–14107.

[29] Das, A., Chakraborty, B., Sood, A. K. "Raman spectroscopy of graphene on different substrates and influence of defects." Bull. Mater. Sci., 2008, 31, 579–584.

[30] Manoj, B., "A comprehensive analysis of various structural parameters of Indian coals with the aid of advanced analytical tools." Int. J. Coal Sci. Technol., 2016, 3, 123–132.

[31] Manoj, B., Kunjomana, A. G., "Systematic investigations of graphene layers in sub-bituminous coal." Russ. J. Appl. Chem., 2014, 87, 1726–1733.

[32] Zhang, S., Liu, Q., Zhang, H., Ma, R., Li, K., Wu, Y., "Structural order evaluation and structural evolution of coal derived natural graphite during graphitization." Carbon, 2020, 157, 714–723.

[33] Ban, F. Y., Majid, S. R., Huang, N. M., Lim, H. N., "Graphene oxide and its electrochemical performance." Int. J. Electrochem. Sci., 2012, 7, 4345–4351.

[34] Rao, C. N. R., Biswas, K., Subrahmanyam, K, S., Govindaraj, A., "Graphene, the new nanocarbon. J. Mater. Chem., 2009, 19, 2457–2469.

[35] Inagaki, M., Intensity ratios between 002 and 004 diffraction lines for various carbons." J. Appl. Crystallogr., 1972, 5, 295–297.

[36] Yue X., Wang, H., Wang, S., Zhang, F., Zhang, R., "In-plane defects produced by ball-milling of expanded graphite." J. Alloys. Compd., 2010, 505, 286–290.

[37] Mohanta, Z., Atreya, H. S., Srivastava, C., "Correlation between defect density in mechanically milled graphite and total oxygen content of graphene oxide produced from oxidizing the milled graphite." Sci. Rep., 2018, 8, 15773.

[38] Zhang, S., Cui, Y., Wu, B., Song, R., Song, H., Zhou, J., Chen, X., Liu, J., Cao, L. "Control of graphitization degree and defects of carbon blacks through ball-milling." RSC Adv., 2014, 4, 505–509.

[39] Fukunaga, T., Nagano, K., Mizutani, U., Wakayama, H., Fukushima, Y., "Structural change of graphite subjected to mechanical milling." J Non Cryst Solids., 1998, 232–234, 416–420.

[40] Welham, N. J., Williams, J. S., "Extended milling of graphite and activated carbon." Carbon, 1998, 36, 1309–1315.

[41] Francke, M., Hermann, H., Wenzel, R., Seifert, G., Wetzig, K., "Modification of carbon nanostructures by high energy ball-milling under argon and hydrogen atmosphere." Carbon, 2005, 43, 1204–1212.

[42] Smolira, A., Szymanska, M., Jartych, E., Calka, A. and Michalak, L., "Structural transformations in graphite induced by magneto-mechanical- milling in hydrogen atmosphere." J. Alloys Compd., 2005, 402, 256–262.

[43] Ferreira, E. M., Moutinho, M. V., Stavale, F., Lucchese, M. M., Capaz, R. B., Achete, C. A. and Jorio, A., "Evolution of the Raman spectra from single-, few-, and many-layer graphene with increasing disorder." Phys. Rev. B-Condens. Matter. Mater. Phys., 2010, 82, 125429.

[44] Gayathri, S., Jayabal, P., Kottaisamy, M. and Ramakrishnan, V., "Synthesis of few layer graphene by direct exfoliation of

[DOI: 10.22068/ijmse.2131]

graphite and a Raman spectroscopic study." AIP Adv., 2014, 4, 27116.
[45] Sole C., Drewett N. E., Hardwick L. J., "In situ Raman study of lithium-ion intercalation into microcrystalline graphite." Faraday Discuss, 2014, 172, 223–237.
[46] P Prasad, B.L.V., Sato, H., Enoki, T., Hishiyama, Y., Kaburagi, Y., Rao, A.M., Eklund, P.C., Oshida, K. and Endo, M., "Heat-treatment effect on the nanosized graphite π-electron system during diamond to graphite conversion." Phys Rev B-Condens. Matter. Mater. Phys., 2000, 62, 11209–11218.
[47] Bokobza L., Bruneel J-L., Couzi M. "Raman Spectra of Carbon-Based Materials (from Graphite to Carbon Black) and of Some Silicone" Composites. C., 2015, 1, 77–94.
[48] Made Joni, I., Vanitha, M., Camellia, P., Balasubramanian, N., "Augmentation of graphite purity from mineral resources and enhancing % graphitization using microwave irradiation: XRD and Raman studies." Diam. Relat. Mater., 2018, 88, 129–136.
[49] Jung, D. W., Jeong, J. H., Cha, B. C., Kim, J. B., Kong, B. S., Lee, J. K., and Oh, E. S. "Effects of ball-milled graphite in the synthesis of SnO_2/graphite as an active material in lithium ion batteries." Met. Mater. Int., 2011, 17, 1021–1026.
[50] Araujo, P. T., Terrones, M., Dresselhaus, M. S., "Defects and impurities in graphene-like materials." Mater. Today, 2012, 15, 98–109.
[51] Teng, C., Xie, D., Wang, J., Yang, Z., Ren, G., Zhu, Y., "Ultrahigh Conductive Graphene Paper Based on Ball-Milling Exfoliated Graphene." Adv. Funct. Mater. , 2017, 27, 1700240.
[52] Antisari, M. V., Montone, A., Jovic, N., Piscopiello, E., Alvani, C., & Pilloni, L., "Low energy pure shear milling: A method for the preparation of graphite nano-sheets." Scr. Mater., 2006, 55, 1047–1050.
[53] Liu, T., Zhang, R., Zhang, X., Liu, K., Liu, Y., Yan, P., "One-step room-temperature preparation of expanded graphite." Carbon, 2017, 119, 544–547.

[DOI: 10.22068/ijmse.2131]